International Journal of Advanced Engineering, Management and Science (IJAEMS)
Peer-Reviewed Journal
ISSN: 2454-1311 | Vol-9, Issue-8; Aug, 2023
Journal Home Page: https://ijaems.com/
Article DOI: https://dx.doi.org/10.22161/ijaems.98.3

Enhancing Flexural Performance of GFRC Square Foundation Footings through Uniaxial Geogrid Reinforcement

El-Sayed A. El-Kasaby[1], Mohab Roshdy[2], Mahmoud Awwad[3], Ahmed A. Abo-Shark[4]*

[1]Prof. of soil mechanics and foundations, Civil Engineering Department, Benha Faculty of Engineering, Benha University, Cairo, Egypt.
[2]Lecturer, Civil Engineering Department, Benha Faculty of Engineering, Benha University, Cairo, Egypt.
[3]Lecturer, Civil Engineering Department, Benha Faculty of Engineering, Benha University, Cairo, Egypt.
[4]Assistant Lecturer, Civil Engineering Department, Benha Faculty of Engineering, Benha University, Cairo, Egypt.
*Corresponding Author

Received: 03 Jul 2023; Received in revised form: 04 Aug 2023; Accepted: 11 Aug 2023; Available online: 18 Aug 2023

Abstract— *This study investigates how the flexural characteristics of square foundation footings, strengthened with glass fiber reinforced concrete (GFRC), are influenced by uniaxial geogrids. The research involves tests on five reinforced concrete square footings under square loading until failure. Variables include geogrid layer count and longitudinal reinforcement proportion. The analysis covers factors like different stage loads, deflection, energy absorption, ductility, and crack patterns. Results indicate that adding geogrid layers with GFRC significantly improves footing flexural performance and fracture mechanism. More geogrid layers lead to notable load increases at each stage. The data also reveals that geogrid reinforced GFRC footings surpass those reinforced with steel and standard concrete mixes in strength resistance. Moreover, a simplified empirical equation correlates footing moment directly to geogrid tensile strength, offering efficient predictive accuracy for their relationship. This research emphasizes uniaxial geogrids' benefits in reinforcing GFRC footings, enhancing flexural performance, and offering valuable insights for earth structure design and construction.*

Keywords— ***Square foundations, Flexural behavior, Geogrid reinforcement, Geosynthetics, Concrete footings, Uniaxial geogrids, Glass fiber reinforced concrete (GFRC).***

I. INTRODUCTION

Due to its flexibility and versatility, reinforced concrete is used a lot in the construction industry. Still, steel reinforcements in concrete that corrosion can cause the structure to weaken and need expensive repairs [1][2]. Researchers are investigating into other materials, such as glass, jute, synthetic coconut fibers, rubber, plastics, sisal, and hemp, to improve the concrete tensile strength [3][4]. Plastics are getting more attention these days because of worries about the environment and the oceans. Even so, they are still used, along with other materials, as reinforcements in civil infrastructure [5][6].

Geogrid, a vital element in geotechnical engineering, plays a significant role in reinforcing and stabilizing civil and infrastructure projects. It can be used instead of or in addition to steel reinforcement, and it works well to reduce the damage caused by impacts [7][8]. Geogrid can be utilized in uniaxial or biaxial forms, depending on the specific application. Uniaxial geogrids are well-suited for slope separators and retaining walls, whereas biaxial geogrids excel in highway structures such as bridges, drainage systems, and pavements [9]. By enabling the construction of steep slopes or walls on weak terrain, geogrids expand the usable land area. Additionally, they reinforce pavements and provide stability to unconsolidated surfaces and asphalt layers [10][11][12].

The utilization of geosynthetic materials in the construction of reinforced concrete (RC) and pavement structures has witnessed a significant surge in recent

decades. Geogrids have become increasingly prevalent in the construction of RC and pavement structures [13]. According to Abdel-Hay (2019) [14], geogrids offer a viable alternative to conventional methods and effectively reinforce RC slabs. The incorporation of geogrids enhances flexural strength and reduces deflection at the failure load. Meski and Chehab [15], as well as Hadi et al. [5], have investigated the potential application of geogrids in reinforcing concrete beams. Their studies have demonstrated that geogrids can markedly improve the strength and flexural capacity of concrete beams. Additionally, experimental studies have demonstrated that the application of geogrids can improve the post-cracking performance, failure mode, strength, and longevity of reinforced structural elements [16][17].

In recent times, there has been an increasing focus on augmenting the strength of concrete by incorporating glass fiber reinforced concrete (GFRC) material [18]. GFRC is recognized for its exceptional durability within concrete and comprises a composite material with a matrix that exhibits an asymmetrical dispersion or arrangement of small fibers, whether they are of natural or synthetic origin [19]. The employment of discrete glass fibers has demonstrated the ability to enhance the shear-friction strength of concrete while serving as an effective shear reinforcement. Additionally, the application of glass fibers has been observed to efficiently mitigate crack propagation in beams and footings [20][21].

The main aim of this study is to examine the flexural properties of square concrete footings that have been strengthened with geogrid reinforcement and GFRC. In this study, four distinct variations of uniaxial geogrids, encompassing both rigid and flexible alternatives, are introduced into footings constructed with glass fiber reinforced concrete (GFRC). The specimens undergo square loading. The experimental results clearly demonstrate that the inclusion of geogrids in the concrete footings significantly enhances both strength and post-cracking ductility, especially when multiple layers of geogrids are used.

II. APPLICATION OF EXPERIMENTS

A- Experimental Design and Samples

In the experiment, five footings with different reinforcement configurations were tested. The footings were square in shape (30 cm x 30 cm x 9 cm) and subjected to specific loading conditions using a 7 cm x 7 cm square loading plate. The footings were divided into five categories to evaluate various reinforcement methods. The control specimen was reinforced with steel without any glass fiber bristles. The other specimens were reinforced with uniaxial geogrid and GFRC, with some having two layers and others having four layers of uniaxial geogrid. Table 1 provides a summary of these configurations.

Table 1: Summary of Experimental Test Conditions

Group Name	Code of Specimen	Reinforced Material	Number of Units	Arrangment of layers	Concrete Mixture
Control	C	Steel	4 @ 6 mm	2 bars on each direction	Reinforced concrete mixture (Without adding fiber bristles)
Geogrid reinforced.	S1	Re 520	4 layers	2 sheets on each direction	Glass fiber reinforced concrete (GFRC)
	S2	Re 570	2 layers	1 sheet on each direction	
	S3	Re 540	4 layers	2 sheets on each direction	
	S4	Re 580	2 layers	1 sheet on each direction	

B- Components of Reinforced Concrete

In our experimental specimens, we used ordinary Portland cement (OPC-42.5 grade), natural sand (fineness modulus of 2.6), and filter stones (maximum aggregate size of 9 mm). The concrete mix comprised carefully measured quantities of key components: 450 kg/m3 of cement, 680 kg/m3 of sand, 215 liters/m3 of water, and 970 kg/m3 of coarse aggregate. The GFRC mix have the same items in addition to 2.5 kg/m3 of 12-16 mm long glass fiber bristles with a diameter of 12 microns, supplied by the CMB Group company in Egypt. The normal reinforced concrete mix achieved a compressive strength of 28 MPa at 28 days, while the glass fiber reinforced concrete (GFRC) had a strength of 32.26 MPa.

C- Footings reinforcement

The experimental control specimen employed standard mild steel bars with a diameter of 6 mm and a grade of 36, possessing a yield stress of 36 Ksi, as the primary reinforcement in both longitudinal and transverse directions (as illustrated in Figure 1-a). Furthermore, uniaxial geosynthetic geogrids, supplied by Tensar International Corporation and imported by National

Geotechnical Company for GEOTECH, were extensively utilized in this research (as referenced in [22]). The mechanical properties of the uniaxial geogrids employed in this research were described in Table 2. Uniaxial Geogrids Re520, Re540, Re570, and Re580 were employed and are depicted in Figures 2-b to 2-e.

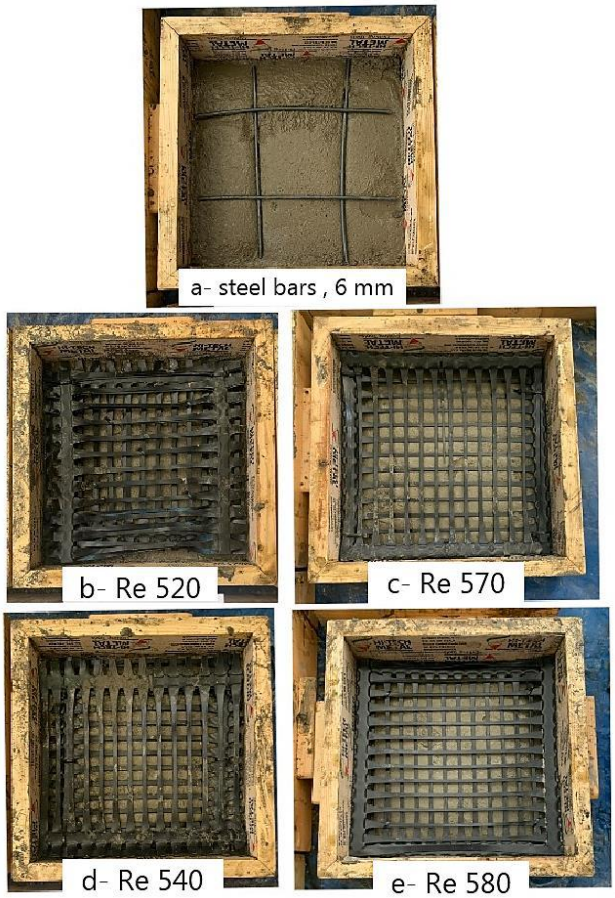

Fig.1: Specimen Reinforcement Layout

Table 2: Uniaxial Geogrid Mechanical Properties Consistent with Manufacturer's Specifications.

Component of Uniaxial geogrid					
Mechanical properties	Uniaxial Geogrid type				Unit
	Re 520	Re 540	Re 570	Re 580	
polymer	High density polyethylene				
Junction strength	95%				
Unit weight	0.36	0.45	0.87	0.98	Kg/m^2
Long term strength	25.10	30.66	56.28	65.27	Kn/m

D- Analysis of Soil Specifications

The soil used in this study was classified as well-graded gravel with sand according to the unified soil classification system. Its grading was determined by the uniformity coefficient (22.50) and uniformity curvature (1.98). The soil's compaction characteristics were evaluated through the standard proctor test, revealing a maximum dry density of 2.078 t/m3 and an optimum moisture content of 6.88%. These test results provide valuable insights into the soil's suitability for the footings' application.

Experimental Setup and Instrumentation Configuration

The laboratory-based study utilized a model setup comprising a sturdy test tank, a loading mechanism, a sensor-equipped plate, and a data collection system. The tank, constructed from rigid steel, had dimensions of 1.50 meters in length, 1.50 meters in width, and 0.70 meters in height, Figure 2-a. A motorized hydraulic jack applied a constant load to the footing, with the load measured using

a 1000 kN capacity load cell placed on top. Five LVDT transducers with a resolution of 0.04 mm were strategically positioned on the footing to capture any vertical displacement. The output voltage from each electrical measuring circuit was automatically recorded at one-minute intervals through a data logging system. Figure 2-b, provided a visual representation of the apparatus, illustrating its principal dimensions and layout, ensuring accurate data acquisition, and facilitating subsequent analysis.

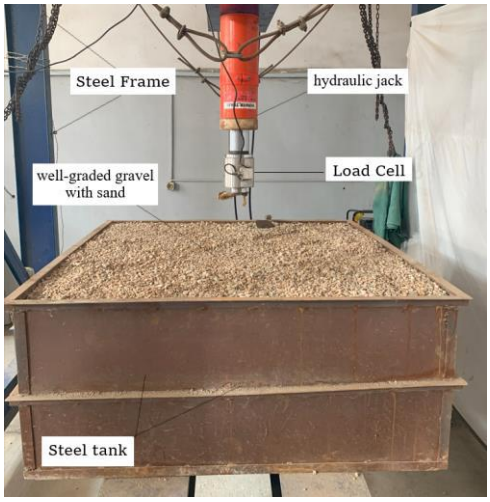

(a) Soil setup inside the steel tank

(b)

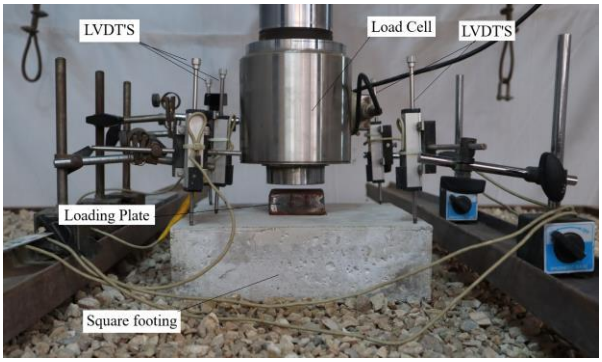

(b) Footing setup for testing

Fig.2: Experimental Setup for footing specimen.

III. FINDINGS AND EVALUATION

Figures 3 depict the load-displacement response of square concrete footings that were enhanced with either two or four layers of uniaxial geogrids. The load-carrying capability (P) and vertical displacement (Δ) were calculated for all the examined footings during the initial crack, yield, and ultimate stages. Moreover, the ductility (μ) and energy absorption (En) properties of each footing were assessed. A comprehensive compilation of these parameters is presented in Table 3.

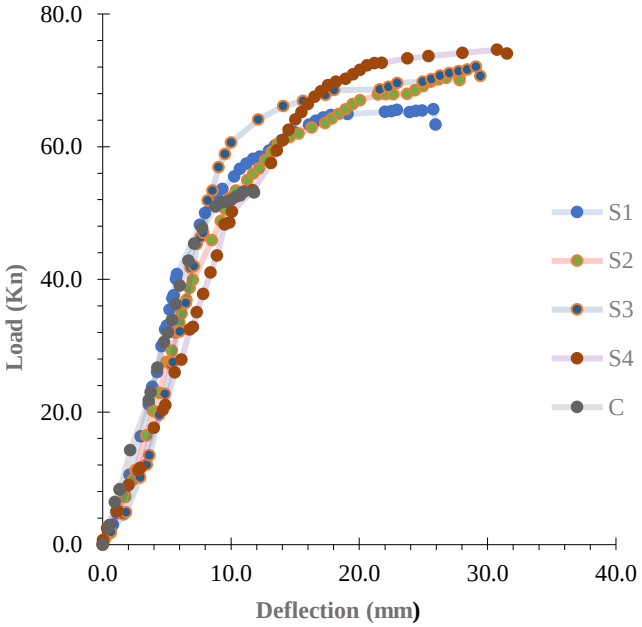

Fig.3. load-deflection relationship of square concrete footings that have been reinforced with both steel and Uniaxial geogrids.

A- Investigating the influence of glass fiber and geogrid on footing performance at various stages.

1- Load Capacity at Various stages

The results suggest that the inclusion of glass fiber bristles and geogrid reinforcement in footings effectively delays the onset of initial cracks, and the post-crack behavior of the reinforced footings exhibits significantly higher load-carrying capacities compared to the square footing (C), as illustrated in Figure 3. Furthermore, when compared to the control footing, the application of uniaxial geogrid reinforcement with GFRC leads to gradual improvements in the cracking load (Pfc), yield load (Py), and ultimate load (Pult).

Footings reinforced with four layers of uniaxial geogrid Re 520 show significant improvements in load capacity. The values of cracking load (P_{fc}), yield load (P_y), and ultimate load (P_{ult}) increase by approximately 21.90%, 19.23%, and 23.32%, respectively, compared to the concrete control footing (C).

Similarly, footings reinforced with two layers of uniaxial geogrid Re 570 exhibit enhanced load-carrying capacities. The values of P_{fc}, P_y, and P_{ult} increase by approximately 22.51%, 28.50%, and 32.45%, respectively, when compared to the concrete control footing (C).

Moreover, footings reinforced with four layers of uniaxial geogrid Re 540 demonstrate significant improvements in load capacity. The values of P_{fc}, P_y, and

P_{ult} increase by approximately 26.82%, 33.10%, and 35.35%, respectively, compared to the concrete control footing (C).

Lastly, footings reinforced with two layers of uniaxial geogrid Re 580 exhibit notable enhancements in load-carrying capacities. The values of P_{fc}, P_y, and P_{ult} increase by approximately 34.14%, 35.79%, and 40.18%, respectively, when compared to the concrete control footing (C).

These findings highlight the effectiveness of incorporating uniaxial geogrid reinforcement in improving the load capacity of footings and suggest that the number of layers and specific geogrid type play a significant role in enhancing the structural performance of the footings.

Table 3: The parameters and properties of square concrete footings that have been reinforced with both steel and Uniaxial geogrids.

	First crack stage		Yield stage		Ultimate load stage		Ductility factor	Energy absorption
	P_f (Kn)	Δ_f (mm)	P_y (Kn)	Δ_y (mm)	P_u (KN)	Δ_u (mm)	μ	En (kn/mm)
C	41.000	7.653	51.000	8.500	53.225	11.044	1.299	398.702
S1	50.000	8.310	60.810	14.400	65.642	25.785	1.791	1309.523
S2	50.230	9.312	65.536	15.530	70.500	27.824	1.792	1409.116
S3	52.000	9.384	67.881	16.110	72.043	29.087	1.806	1591.158
S4	55.000	12.312	69.253	16.900	74.615	30.738	1.819	1704.215

2- Vertical displacement Across Different stages

When compared to a control footing (C), the footings reinforced with uniaxial geogrid and glass fiber bristles demonstrate an increase in vertical displacement values at the cracking stage (Δ_{fc}), yield stage (Δ_y), and ultimate stage (Δ_{ult}), as observed in the load-deflection curves. The specific increases are outlined as follows:

For footings reinforced with four layers of uniaxial geogrid Re 520, the values of Δ_{fc}, Δ_y, and Δ_{ult} increase by approximately 8.58%, 69.41%, and 133.47%, respectively, compared to the concrete control footing (C). Similarly, footings reinforced with two layers of uniaxial geogrid Re 570 exhibit increases in Δ_{fc}, Δ_y, and Δ_{ult} values of about 21.67%, 82.70%, and 151.9%, respectively, in comparison to the concrete control footing (C).

Furthermore, footings reinforced with four layers of uniaxial geogrid Re 540 demonstrate increases in Δ_{fc}, Δ_y, and Δ_{ult} values of approximately 22.61%, 89.52%, and 163.36%, respectively, compared to the concrete control footing (C). Lastly, footings reinforced with two layers of uniaxial geogrid Re 580 exhibit significant increases in Δ_{fc}, Δ_y, and Δ_{ult} values, with approximately 60.87%, 98.82%, and 178.32% increases, respectively, in comparison to the concrete control footing (C).

B- Energy Absorption [En].

The ability to absorb high levels of energy is crucial, especially in scenarios such as major earthquakes, where effective dissipation of energy is required to mitigate significant dynamic responses and provide sufficient hysteretic damping in concrete structures. The energy dissipation capability of the footings under investigation was assessed by calculating the area enclosed by their load-deflection curves, as depicted in Figure 3. Furthermore, a comparative analysis of the footings was conducted based on their energy absorption capacity, revealing the following observations.

The energy absorption for S1 exhibited a substantial increase of approximately 228.44% compared to the concrete control footing (C). Similarly, the energy absorption for S2 demonstrated a significant increase of about 253.42% compared to the concrete control footing (C).

Furthermore, the energy absorption for S3 showed a remarkable increase of approximately 299.08% compared to the concrete control footing (C). Additionally, the energy absorption for S4 displayed a substantial increase of about 327.441% compared to the concrete control footing (C).

These findings highlight the significant improvements in energy absorption achieved by the respective configurations (S1, S2, S3, and S4) when compared to the concrete control footing.

C- Displacement Ductility Factor [μ]

In this study, we examined the influence of geogrid reinforcement on the displacement ductility characteristics of concrete footings. The displacement ductility index, which measures the ability of structural elements to

withstand considerable deflections without experiencing significant loss in strength prior to failure, was employed to assess the performance of the concrete footings. Maintaining the strength of concrete structures above the yield strength and allowing for permissible plastic deformation, as specified in the design guidelines [21], is essential to ensure their resilience during seismic events.

The Displacement Ductility factor for S1 demonstrated a substantial increase of approximately 37.81% compared to the concrete control footing (C). Similarly, the Displacement Ductility factor for S2 exhibited a notable increase of about 37.9% compared to the concrete control footing (C). Furthermore, the Displacement Ductility factor for S3 displayed a significant increase of approximately 39% compared to the concrete control footing (C). Additionally, the Displacement Ductility factor for S4 showcased a remarkable increase of about 40% compared to the concrete control footing (C).

These findings highlight the substantial enhancements in Displacement Ductility achieved by the respective configurations (S1, S2, S3, and S4) when compared to the concrete control footing. Furthermore, our investigation unveiled a direct association between the augmentation in displacement ductility and the tensile strength of the utilized uniaxial geogrids. Additionally, the inclusion of multiple layers of uniaxial geogrid reinforcement did not detrimentally impact the response of the footings, as evidenced by the load-deflection curves. Consequently, the integration of multiple layers of uniaxial geogrid reinforcement presents a pragmatic and efficient approach to enhance the overall performance of reinforced concrete footings.

D. Failure Mechanism

In the conducted tests on the concrete footings, crack development was observed to predominantly occur in a perpendicular direction to the load plate. Specifically, flexural cracks were observed, while shear cracks were absent. The failure pattern of the concrete footings was characterized by the widening of cracks, the appearance of additional cracks in certain footings, and the propagation of these cracks from the tension zone (located at the bottom surface of concrete) to the compression zone (located at the top surface of concrete), ultimately leading to failure.

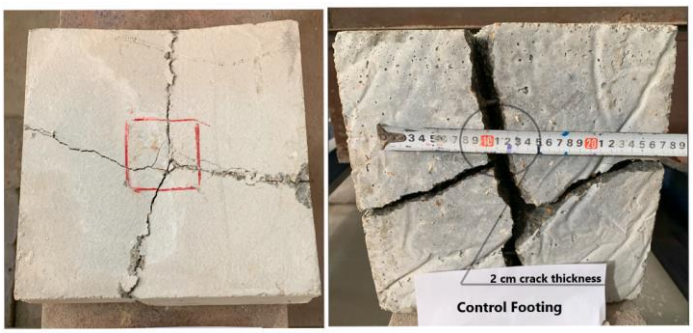

a- Control footing

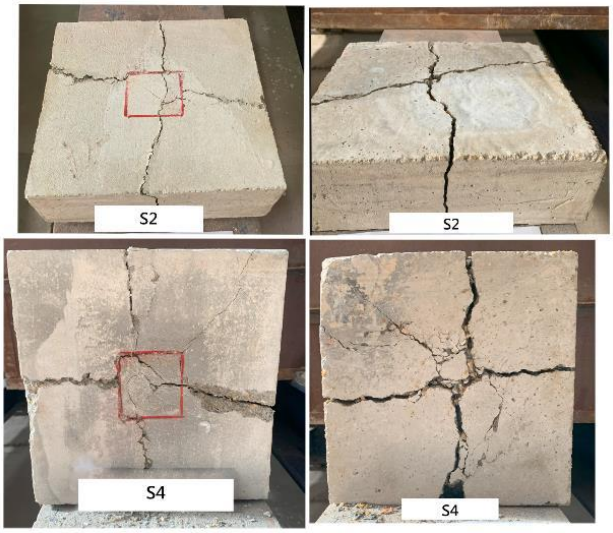

b- Footings with two uniaxial layers, S2 and S4

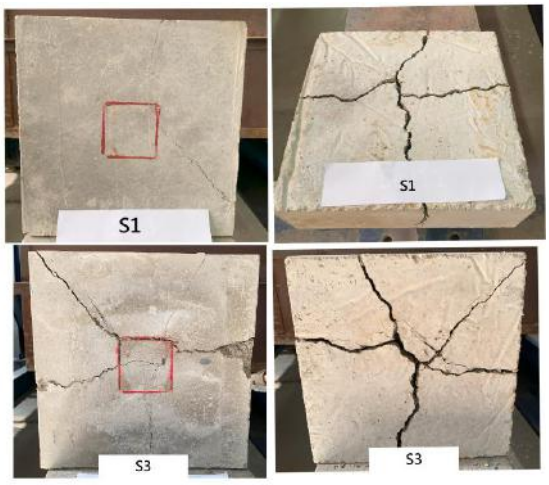

c- Footings with four uniaxial layers, S1 and S3

Fig.4: The observed crack patterns in the concrete footings.

Within the control concrete footing (C), four noticeable cracks emerged and progressively extended until reaching failure. These cracks exhibited notable width, signifying

significant impairment to the steel reinforcement bars upon reaching the load capacity that caused failure, Figure 4-a.

In contrast, the concrete footing reinforced with two layers of uniaxial geogrid exhibited the presence of multiple smaller cracks, which were observed to propagate in various directions (Figure 4-b). These cracks displayed narrower widths, and their density notably decreased in footings reinforced with four layers of geogrid compared to those reinforced with two layers (Figure 4-c). Importantly, no evidence of rib cutting was observed in the uniaxial geogrids. Overall, the damage observed in the samples reinforced with uniaxial geogrids was significantly milder in comparison to the damage observed in the control samples. Thus, a direct correlation can be observed between the quantity and width of flexural cracks, the tensile strength of geogrids, and the number of geogrid layers, as indicated by the findings of this research.

E. Correlation between Square Footing Moment and Geogrid Reinforcement

The study aims to explore the relationship between the applied moment on a square footing and the effectiveness of using uniaxial geogrids as reinforcement. By analyzing various factors such as load distribution and geogrid properties. The findings of this analysis will contribute to a better understanding of the interaction between footing moments and geogrid reinforcement, aiding in the development of more efficient and reliable geotechnical design practices.

The calculation of the ultimate moment (Mu) and the required area of geogrid (Ag) for all groups of square footings has yielded conclusive results, Fig. 5. In order to establish a correlation between the ultimate moment (Mu) and the required area of geogrid (Ag) for different square footings (S 1 to S 4), data-fit software was employed. This software allowed for the analysis of the relationship between M_u and A_g. Consequently, an empirical formula can be derived from these results as given in (Eq.1).

$$Ag = \delta * e^{\sigma * \frac{Mu}{d}} = N * L * \quad T_{ult} \qquad (1)$$

In the provided context, the variables in the equation have specific meanings. Here are their explanations:

- Ag: Total ultimate strength of the uniaxial geogrid on the square footing (Kn).
- Mu: Ultimate moment exerted on the footing (Kn.m).
- d: Depth of the square footing (m).
- δ: Value of 3 for reinforced concrete mixture and 2.1608 for glass fiber reinforced concrete mixture (Constant values).
- σ: Value of 0.106 for reinforced concrete mixture and 0.1204 for glass fiber reinforced concrete mixture (Constant values).
- N: Number of geogrid layers.
- L: Length of geogrid within the footing (m).
- T_{ult}: Tensile strength of the uniaxial geogrid used (Kn/m).

These points provide a concise overview of the variables and their respective meanings.

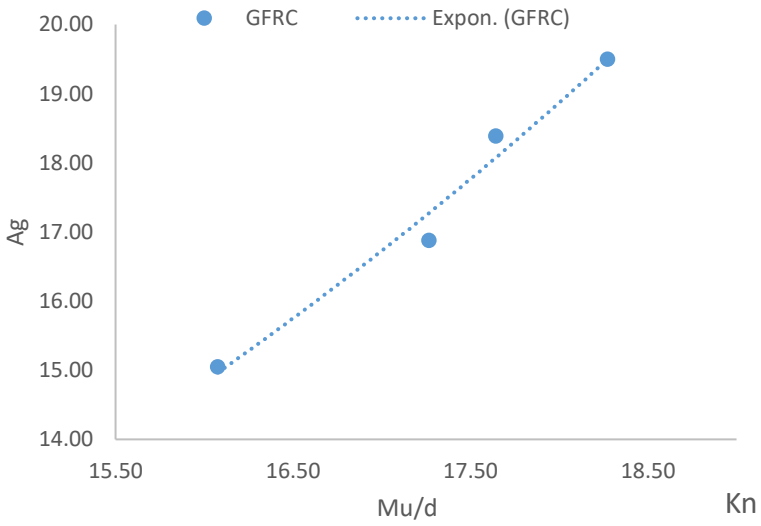

Fig. 5: Correlation between (Mu/d) and Required Area of uniaxial Geogrid (Ag) for Different footings.

IV. CONCLUSION

1- Uniaxial geogrid reinforcement with GFRC significantly enhances the load capacity of footings, with improvements in cracking load (P_{fc}), yield load (P_y), and ultimate load (P_{ult}) ranging from approximately 19.23% to 40.18% compared to the concrete control footing.

2- Geogrid reinforcement substantially improves the displacement ductility of footings, with notable increases in Δ_{fc}, Δ_y, and Δ_{ult} values ranging from approximately 8.58% to 178.32% compared to the concrete control footing.

3- Geogrid reinforcement leads to substantial improvements in energy absorption capacity, with increases ranging from approximately 228.44% to 327.441% compared to the concrete control footing.

4- Geogrid reinforcement positively impacts the Displacement Ductility factor, with increases ranging from approximately 37.81% to 40%, enhancing the structural element's capacity to endure significant deflections without strength reduction.

5- Geogrid reinforcement effectively mitigates crack development, reducing crack width and damage to steel bars, improving the overall structural integrity of the concrete footings.
6- An empirical formula was developed to establish a relationship between the ultimate moment (M_u) and the required area of geogrid (A_g) for square footings.

In summary, the study highlights the significant benefits of utilizing uniaxial geogrid reinforcement in enhancing the load capacity, displacement ductility, energy absorption, and crack mitigation in concrete footings. These findings contribute to the advancement of engineering practices and offer valuable insights for designing and constructing resilient structures in various applications.

REFERENCES

[1] Banu ST, Chitra G, Awoyera PO, Gobinath R. Structural retrofitting of corroded fly ash based concrete beams with fibres to improve bending characteristics. Australian Journal of Structural Engineering. 2019 Jul 3;20(3):198-203.

[2] Tharani K, Mahendran N, Vijay TJ. Experimental investigation of geogrid reinforced concrete slab. Int J Innov Technol Explor Eng. 2019;8(6):88-93.

[3] Asim M, Uddin GM, Jamshaid H, Raza A, ul [Rehman Tahir] Z, Hussain U, et al. Comparative experimental investigation of natural fibers reinforced lightweight concrete as thermally efficient building materials. J Mater Res Technol. 2020;9(2):1753-1763.

[4] Sanjeev J, Nitesh KS. Study on the effect of steel and glass fibers on fresh and hardened properties of vibrated concrete and self-compacting concrete. Materials Today: Proceedings. 2020 Jan 1;27:1559-68..

[5] Hadi MNS, Al-Hedad ASA. Flexural fatigue behaviour of geogrid reinforced concrete pavements. Constr Build Mater. 2020;249:118762.

[6] Meng X, Chi Y, Jiang Q, Liu R, Wu K, Li S. Experimental investigation on the flexural behavior of pervious concrete beams reinforced with geogrids. Constr Build Mater. 2019;215:275-284.

[7] Jallu M, Arulrajah A, Saride S, Evans R. Flexural fatigue behavior of fly ash geopolymer stabilized-geogrid reinforced RAP bases. Constr Build Mater. 2020;254:119263.

[8] Tang X, Higgins I, Jlilati MN. Behavior of Geogrid-Reinforced Portland Cement Concrete under Static Flexural Loading. J Mater Civ Eng. 2019;31(3):04018399.

[9] Chen C, McDowell GR, Thom NH. Investigating geogrid-reinforced ballast: experimental pull-out tests and discrete element modelling. Soils Found. 2014;54:1-11..

[10] Abdesssemed M, Kenai S, Bali A. Experimental and numerical analysis of the behavior of an airport pavement reinforced by geogrids. Constr Build Mater. 2015;94:547-554.

[11] Tang X, Higgins I, Jlilati MN. Behavior of Geogrid Reinforced Portland Cement Concrete under Static Flexural Loading. Infrastructures. 2018;3(4):41.

[12] El-Kasaby EA, Eissa EA, Ab-Elmeged MF, Abo-Shark AA. Coefficient of Consolidation and Volume Change for 3-D Consolidation. European Journal of Engineering and Technology Research. 2019 May 25;4(5):126-31.

[13] Radnic J, Matesan D, Grgic N, Baloevic G. Impact testing of RC slabs strengthened with CFRP strips. Compos Struct. 2015;121:90-103.

[14] Gabr ASAH. Strengthening of Reinforced of Concrete Slabs Using Different Types of Geo-grids. Int J Civ Eng Technol (IJCIET). 2019;10(1):1851-1861.

[15] El Meski F, Chehab GR. Flexural behavior of concrete beams reinforced with different types of geogrids. J Mater Civ Eng. 2014;26(8):04014038.

[16] Pant A, Datta M, Ramana GV, Bansal D. Measurement of role of transverse and longitudinal members on pullout resistance of PET geogrid. Meas. 2019;148:106944.

[17] Tam AB, Park D-W, Le THM, Kim J-S. Evaluation on fatigue cracking resistance of fiber grid reinforced asphalt concrete with reflection cracking rate computation. Constr Build Mater. 2020;239:117873.

[18] Tahir M, Wang Z, Ali KM, Isleem HF. Shear behavior of concrete beams reinforced with CFRP sheet strip stirrups using wet-layup technique. Struct. 2019;22:43-52.

[19] Ali B, Qureshi LA. Influence of glass fibers on mechanical and durability performance of concrete with recycled aggregates. Constr Build Mater. 2019;228:116783.

[20] Siva Chidambaram R, Agarwal P. The confining effect of geo-grid on the mechanical properties of concrete specimens with steel fiber under compression and flexure. Constr Build Mater. 2014;71:628-637.

[21] El-Kasaby EA, Awwad M, Roshdy M, Abo-Shark AA. Behavior of Square footings reinforced with glass fiber bristles and biaxial geogrid. European Journal of Engineering and Technology Research. 2023 June 25;8(4):5-11.

[22] Tensar International Corporation and imported, 2500 Northwinds Parkway, Suite 500 Alpharetta, GA 30009, Tel. (770) 344-2090 Email: info@tensarcorp.com, web. https://www.tensarcorp.com/solutions/geogrids/triax.